

# Disaster Feature Classification on Aerial Photography to Explain Typhoon Damaged Region using Grad-CAM

Yasuno Takato<sup>1</sup>

<sup>1</sup> Yachiyo Engineering Co., Ltd., Asakusabashi 5-20-8, Taito-ku, Tokyo, Japan  
tk-yasuno@yachiyo-eng.co.jp

**Abstract.** Recent years, typhoon damages has become social problem owing to climate change. Especially, 9 September 2019, Typhoon Faxai passed on the south Chiba prefecture in Japan, whose damages included with electric and water provision stop and house roof break because of strong wind recorded on the maximum 45 meter per second. A large amount of tree fell down, and the neighbour electric poles also fell down at the same time. These disaster features have caused that it took eighteen days for recovery longer than past ones. Initial responses are important for faster recovery. As long as we can, aerial survey for global screening of devastated region would be required for decision support to respond where to recover ahead. This paper proposes a practical method to visualize the damaged areas focused on the typhoon disaster features using aerial photography. This method can classify eight classes which contains land covers without damages and areas with disaster, where an aerial photograph is partitioned into 4,096 grids that is 64 by 64, with each unit image of 48 meter square. Using target feature class probabilities, we can visualize disaster features map to scale the colour range from blue to red or yellow. Furthermore, we can realize disaster feature mapping on each unit grid images to compute the convolutional activation map using Grad-CAM based on deep neural network layers for classification. This paper demonstrates case studies applied to aerial photographs recorded at the south Chiba prefecture in Japan after typhoon disaster. (247 words)

**Keywords:** Typhoon Disaster Response, Aerial Survey, Classification, Grad-CAM, Damaged Feature Mapping.

## 1 Objective

### 1.1 Related works and papers

**Aerial Survey for Natural Disaster Monitoring.** In order to recognize a status after natural disaster, several aerial surveys are available from various height overview such as satellite imagery, aircraft, helicopter, and drone. There are many related works around the devastated area where some disaster occurred at each phase of preparedness, urgent response, and recovery.

Chou et al.[1] proposed the drone-base photographing workflow for disaster monitoring and management operation to get real-time aerial photos. Here, the digital camera had 21 million pixels on the focal distance 1.8mm. They analysed the overall environment

change caused by the MORAKOT typhoon hit on the south Taiwan 2009, whose accumulation of rainfall depth is 2583mm, 91 hours. After the image rectification process, they estimated the new collapse and landslides for reference of emergency rescue. A digital photogrammetry were applied on the camera to produce the digital terrain model data of 5m resolution. The pro of drone use is to overcome transport barriers to quickly acquire all the major affected area of the real-time disaster information. But, the con is that drone is not able to keep a long flight more than 30 minutes.

The JICA survey team [2] used a helicopter owned by the air force of Sri Lanka to investigate the flood and sediment disaster damages caused by the strong winds and the heavy rainfalls during 15 to 18 May 2016, named as Cyclone Roanu. That made a result in the number of death 89 people and missing 102 people, and expanded its landfall in the boundary area between Bangladesh and India. They also collected the Light Detection and Ranging (LiDAR) data to compare between before normal status and after landslide. The aerial photograph could visualize the damages where roads are flooded, river water exceeded a dike in residential areas, landslide or collapse, debris flow on the top of mountain. Focusing on the landslide area, they made several orthophoto images by LiDAR survey with the 0.5m resolution, and by Advanced Land Observing Satellite (ALOS) with the 5.0m resolution, and the Shuttle Radar Topography Mission (SRTM) with the 30m resolution. And they also classified the slope angle degree ranged colour from green to red. This project focused on the hazard of landslide to grasp the affected area after cyclone using the use of helicopter and several satellite imagery resources. The advantage of LiDAR is that beside rain and clouds, no other weather conditions limit their use [3]. As an active sensor, missions in the night-time are possible. In Japan, there is a Bosai platform [4] for disaster preparedness, response and recovery. Several private company [5][6] have investigated after natural disaster using aerial survey and made a disaster mapping for emergency use.

However, it takes high cost of satellite image over global viewpoint and it needs longer time to get a target image of fully covered region. On the other hand, drone surveillance takes lowest cost though the flight time is twenty or thirty minutes, and the scope is narrow due to the constraint of height available flight. This paper focuses on the aerophotographs because it is reasonable cost more than satellite imagery and it has advantage of global sky view more than drone images.

**Disaster Damage Assessment and Feature Extraction.** First, there are a lot of earthquake damage detection especially building damage using satellite imagery, LiDAR point clouds, drone images, and so forth. For example, He et al. [7] presented 3D shape descriptor of individual roofs for detecting roofs with surface damage and roof exhibiting structural damage. Their experiments using post-event airborne LiDAR point clouds of the 2010 Haiti earthquake, whose average point clouds density is 3.4 points per square meter. However, it is not always possible to acquire an airborne LiDAR data of devastated region to be full-covered after each disaster. This approach would take too high cost to prepare the input data source for damage assessment. On the other hand, the increasingly widespread availability of inexpensive drone platforms has driven recent adoption for search and rescue operations. Nex et al. [8] presented a method to autonomously map building damages with a drone in near real-time. They integrated two components that allow the live streaming of images on a laptop and their processing on the drone fly. Though they carried out two pilot test, the dataset were acquired over

a building demolition site of two district in France, where the flight height is only 50m. Unfortunately, this study is too narrow experience to explore the practical use for disaster response. The limitation of method based on drone is also the short flight time less than 30 minutes in order to search the devastated region completely covered.

Next, regarding typhoon damage assessment, Liu et al. [9] reported the Landsat-8 automatic image processing system (L-8 AIPS) which enables to the most up-to-date scenes of Taiwan to be browsed, and in only one hour's time after receiving the raw data from United States Geological Survey (USGS) level-1 product. Using this application, all historical Landsat-8 images in Taiwan could be quickly viewed in time series at the 15m full resolution. They demonstrated that the gap between the user's needs and the existing level-1 product can be bridged by providing browsable images in near real-time. The successful examples contained with the debris flow triggered by Typhoon Souderlor (8 August 2015), and the barrier lake formed and the large-scale destruction of vegetation after Typhoon Nepartak (7 July 2016). However, this application depended on the specific satellite imagery and each country must customize such an application, the limitation is the 15m resolution for monitoring disaster damages.

Furthermore, Sheykhmousa et al. [10] focused on the post-disaster recovery process before typhoon and after four years, and they classified the five classes of land cover and land use changes to visualize the recovery map which enables to signal positive recovery, slightly positive, neutral, slightly negative, and negative recovery. They suggested that their method is created for post-disaster recovery assessment based on multi-temporal and high-resolution satellite images at the 2m resolution. They analysed and evaluated different trajectories of change and transition patterns which signal positive or negative recovery. They studied on three World View-2 images acquired over Tacloban city, Philippines, which was heavily affected by Typhoon Haiyan in 2013, where 2678 people died. The customized hierarchical definition of land cover and use classes were categorized into three parent groups such as built-up, vegetation, and water in Tacloban. Natural forces are heavy winds, storm surges, and destroyed existing urban facilities. Regarding building, though mainly two damage classes can be distinguished into rubble and debris, at the city scale and with the 2m resolution, it was not possible to distinguish debris from rubble, and then these two classes were merged into one class. The other two damage classes contained with inundated land and flattened trees. The machine learning algorithms such as support vector machine, a robust one were employed with texture features extracted from the grey level co-occurrence matrix and local binary patterns. They demonstrated a land cover and land use recovery map that quantify the post-disaster recovery process at the pixel level, and found that physical and functional recovery can be mainly expressed through the land cover and land use change information. Unfortunately, this study is not initial short recovery but four years long recovery process. The classified recovery map is too far view based on satellite imagery at the 2m resolution to extract the damage feature in more detail.

## **1.2 Typhoon Damage Prediction for Initial Response and Faster Recovery**

Thus, one of typhoon disaster features is not clearly explored, especially the complex features contains the tree-fallen and the house roof break. First, the tree-fallen feature

has green-colour of leaves and blown-colour of blanches, so this region of interest is completely colour segmented using the straight forward colour slicing and the standard image processing. Second, it seems that the shape is various owing to the damage intensity of tree-fallen range from light level to extremely one. More flexible learning methods are required for disaster features extraction using deep neural networks.

Initial responses towards typhoon damages are practically important for faster recovery which consists with building damage and electric stop caused by tree-fallen. Therefore, more reasonable sky view screening of devastated region is required for decision support to respond where to prioritize recovery actions. An advantage of aerial photograph is higher resolution that is 0.2m, than satellite imagery and it also enables to wider search efficiently than drone flight. This paper proposes a method to predict the damaged area focused on the typhoon disaster features using aero-photograph images.

## 2 Modelling

### 2.1 Partition Clips and Learning Disaster Features

**Prepare 64 by 64 Partitioned Clips Divided 14K by 15K pixels into 221 by 243.**

Fig. 1 shows a proposed machine learning workflow that consist of the former part of disaster damaged annotation and the later part of classification modelling. First, the size of aero-photographs is 14 thousands by 15 thousands pixels, so the original size is too large and it is not fitted as the input of deep neural networks whose size is frequently 224 by 224 and 229 by 229. High quality learning requires to keep the original RGB data per pixel without resize as far as we can. Therefore, this method make a set of base partitions 64 by 64 into each unit grid image clips with 221 by 243 pixel size. This aerial photograph has the 0.196m resolution so that the real size of unit grid square stands for 44 by 48 meter distance.

**Table 1.** Hierarchical Classes Setting including Land Covers and Typhoon Features

1 residential area (without damage)	5 farm field (rice, crop)
2 house roof break (remained vinyl seat)	6 industrial area (manufacturing)
3 wooded field (without damage)	7 water cover (sea, river, lake)
4 tree fallen field (caused by strong wind)	8 cloudy cover (partial or full)

**Efficient Annotation via Semi-supervised Prediction using Pre-trained Classifier.**

This paper highlights on the typhoon disaster feature such as tree-fallen and house roof break and normal land covers without damages. Table 1 shows a proposed hierarchical eight classes which contains six land covers and two disaster features. We could use 26 images of aerial photograph. Total amount of clip images is almost always very large more than hundred thousands, so human annotation by hands is difficult to divide subgroup of land cover and disaster feature classes. Owing to the hurdle of efficient learning, firstly, we propose to train a base classifier using twenty percent of clip images with the order of twenty thousand images. Secondly, using remained clips with order of eighty thousands as the added input for semi-supervised learning, we can predict the

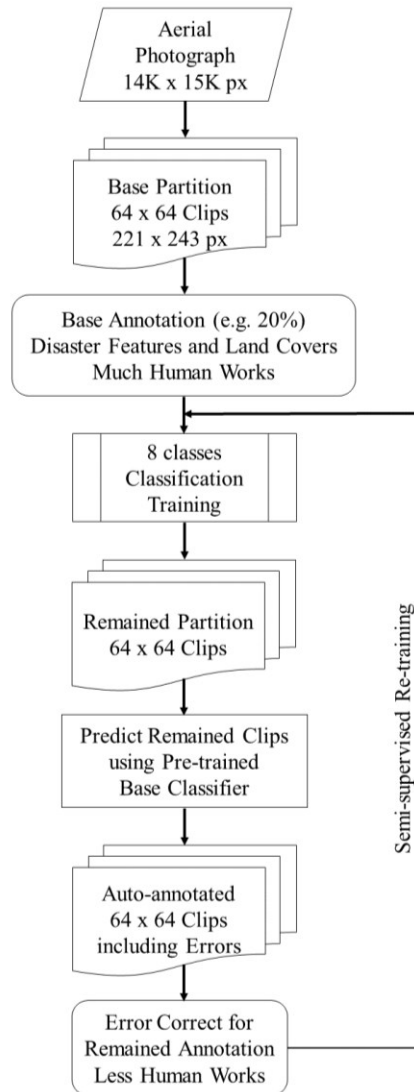


**Fig. 1.** A Machine Learning workflow of Disaster Damaged Annotation and Classification

label per clip and it takes less works of annotation because almost labels are correct and error corrections are less than the case without pre-trained model. And then using the classified labels, we can almost automate to divide their clips into eight subfolders efficiently. Thirdly, human check is possible whether each subfolder contains errors or not, and can correct their miss-classification of clips less works than fully human works.

#### **Accuracy Comparison with Deep Neural Networks.**

We trains classification models base on ten candidates of deep neural networks with advantage of the whole accuracy and two disaster classes of accuracies, that is house

roof break and tree fallen. We propose and compare usable deep neural networks such as AlexNet [11], VGG16 [13], GoogleNet, Inception-v3 [14], ResNet50, ResNet101 [15], Inception-ResNet-v2 [16], DenseNet-201 [17]. Furthermore, MobileNet-v2 [18] and ShuffleNet [19,20] has less parameters and fitted to mobile devices, where the later network uses special techniques such as channel shuffle and group convolution. We can evaluate their accuracy with both recall and precision to compute their confusion matrix. Here, the recall is more important than precision because we should avoid miss-classification in spite of that it contains disaster features.

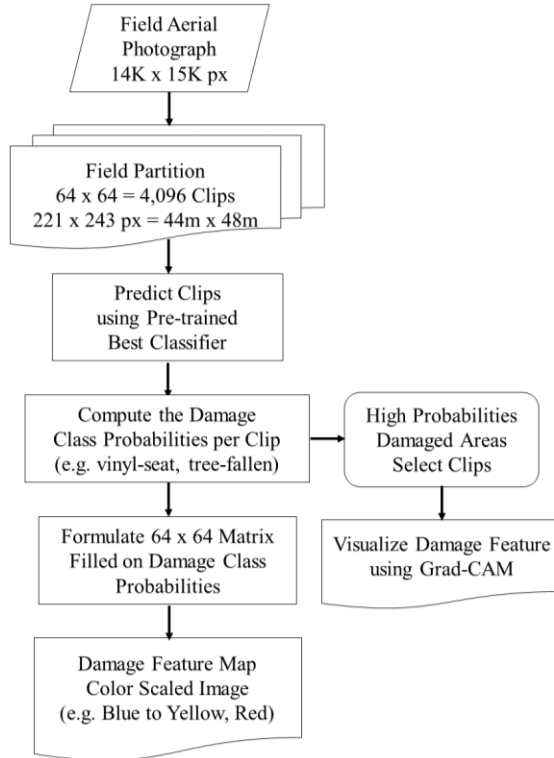


**Fig. 2.** An application workflow for Damaged Feature Mapping Filled on Class Probabilities and for Visualized Damage Feature per Clip Area computing the Grad-CAM

## 2.2 Visual Explanation toward Disaster Features

**Colour Scaled Feature Map using Target Class Probabilities.** Fig 2 shows an application workflow for damaged feature mapping filled on damaged class probabilities and for visualized damage feature per clip area computing the Grad-CAM [21]. Base on the already trained best classifier, we can compute target class probabilities per unit grid, and then we can formulate the damage feature matrix which consists 64 rows and 64 columns. Therefore, we enable to scale the matrix of specific class probabilities into colour feature map ranged among two colours [22]. This paper realize two damage feature map. First, we can create a house roof break feature map to scale colour range

from blue to red. In other words, the house roof break feature can denote the surface of roof covered with vinyl seat on the recovery process within two weeks. The colour range of damage feature map indicate that the blue side is weak damage, the red side is strong damage. Second, we can formulate a tree fallen feature map to scale colour range from blue to yellow. The yellow side is huge damage, the blue side is small damage.

**Visual Disaster Explanation per Unit Grid using Grad-CAM.** In case that some grid area has a high probability at a specific damage class, we can create the micro damage feature map for more detailed scale per unit grid area. We can explain the damage features on each unit grid images to compute the convolutional activation map using Grad-CAM based on deep classification network layers with optimized parameters.

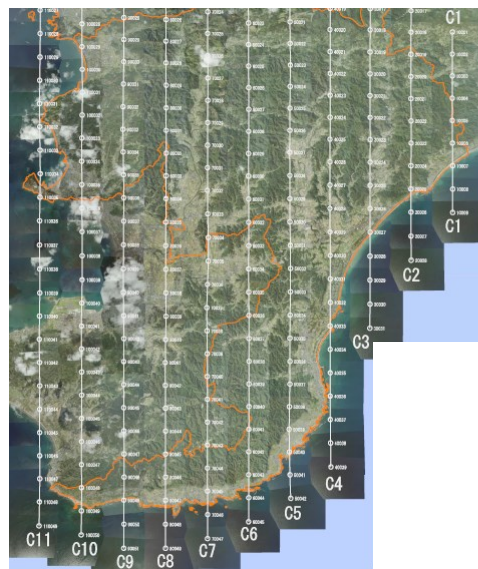


**Fig. 3.** The flight course of Aerial photograph at the south Chiba region acquired on the day 27 to 28 September 2019, provided by Aero Asahi Co.Ltd.

### 3 Applied results

#### 3.1 Training and Test Dataset of Aerial-photographs

This paper demonstrates training and test studies applied to aero-photographs with the size of 14 thousands pixels by 15 thousands ones recorded at the south Chiba region after eighteen days at the post typhoon disaster, 27 to 28 September 2019. Fig. 3 shows the flight course of Aerial photograph at the south Chiba region acquired on the day 27 to 28 September 2019, provided by Aero Asahi Co.Ltd. Here, the real size per pixel on the land is 19.6 cm so that the real size of unit grid square contains 44 by 48 meter distance. The height to get aero-photographs is 3,270 meters and the number of them is 452 images. The number of clip images is 5,954 for a base classifier training at the region of Kimitsu city on the middle Chiba prefecture. Here, we set the division of train

and test is 7 : 3. Several test aero-photographs are located at the region of Kyonan town and Tateyama city on the south Chiba prefecture.

### 3.2 Damage Feature Classifier Trained Results

The author applied to ten classification deep neural networks as base model towards the number of 5954 of unit grid clips, which are divided into rates with training 70 and 30 test. Transfer learning is useful for faster training and disaster response. Here, the author make freeze the round 70 to 80 percent of deep network layers at the concatenation point combined with convolutional layers and skip connections. Table. 2 indicates the accuracy comparison between ten deep neural networks, which has each number of whole layers setting with the frozen layer point. In this study, the mini-batch size is 32, and the maximum epoch is 30 with shuffle every epoch. One epoch has 130 iterations. Further, the initial learning rate is 0.0005, and learning rate schedule is every 5 epoch with drop factor 0.75. Fig. 4 shows the training process of log-loss function with 3000 iterations. From computing results, the ShuffleNet has the most accurate for 30 percent test clips validation. Furthermore, on ShuffleNet the damage class accuracy of both recall and precision has higher score than other nine deep neural networks. Table. 3 shows the confusion matrix of the most promising ShuffleNet.

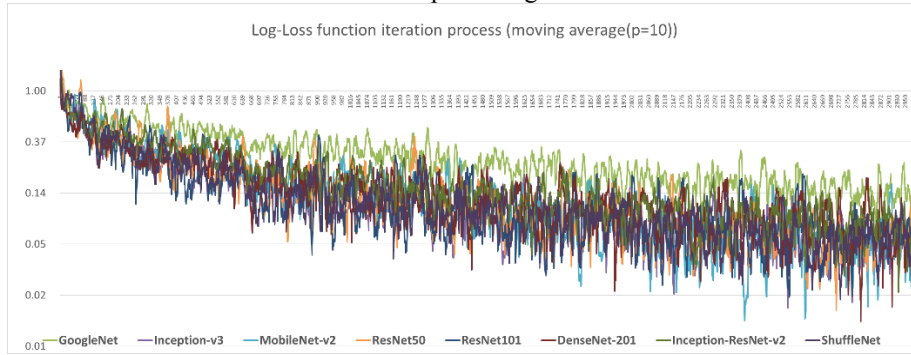


Fig. 4. Compared training process of log-loss function (moving average from 10 iterations)

Table 2. Accuracy comparison between various models

CNN models	Total validation accuracy	house roof break (covered vinyl-seat) accuracy		tree-fallen accuracy		Frozen layer /Whole layer	Runing time (minutes)
		recall	precision	recall	precision		
AlexNet	89.59	67.9	97.6	95.8	68.8	16/25	20
VGG16	88.07	66.3	89.9	87.8	71.2	32/41	50
GoogleNet	89.75	<b>78.6</b>	92.7	93.1	69.5	110/144	27
Inception-v3	90.26	70.1	97.7	<b>99.9</b>	66.1	249/315	79
MobileNet-v2	88.63	64.6	98.1	<b>99.6</b>	65.6	104/154	38
<b>ResNet50</b>	<b>90.48</b>	<b>74.5</b>	96.8	<b>99.6</b>	<b>74.1</b>	120/177	46
ResNet101	88.02	63.8	<b>98.7</b>	<b>99.6</b>	69.1	290/347	70
<b>DenseNet-201</b>	<b>92.16</b>	<b>75.3</b>	96.3	97.7	<b>77.1</b>	647/708	193
Inception-ResNet-v2	88.52	69.5	<b>98.3</b>	95.1	<b>74.3</b>	766/824	175
<b>ShuffleNet</b>	<b>93.39</b>	<b>82.3</b>	<b>98.1</b>	<b>98.9</b>	<b>79.7</b>	137/172	33

**Table 3.** Confusion matrix of the ShuffleNet best classifier (row : truth, column : prediction)

1residencialN851	247	4			4				96.9%	3.1%
2vinylSeatN811	15	200	4	16	8				82.3%	17.7%
3woodedN752	1		177	48					78.3%	21.7%
4treeFallenN872			3	259					98.9%	1.1%
5farmN846	5		3	2	244				96.1%	3.9%
6industrialN691						207			100.0%	
7seaN517			4				151		97.4%	2.6%
8cloudyN614	1							183	99.5%	0.5%
	91.8%	98.0%	92.7%	79.7%	95.3%	100.0%	100.0%	100.0%		
	8.2%	2.0%	7.3%	20.3%	4.7%					
	1residencialN851	2vinylSeatN811	3woodedN752	4treeFallenN872	5farmN846	6industrialN691	7seaN517	8cloudyN614		

### 3.3 Damage Feature Map and Unit Grid Visualization Results

Fig. 5 shows the tree-fallen damage feature map based on the class probabilities per clip. The colour is scaled between the blue and yellow. The yellow side is positive tree-fallen caused by strong wind. Here, we can understand that a lot of tree-fallen areas are located besides river and around mountain.

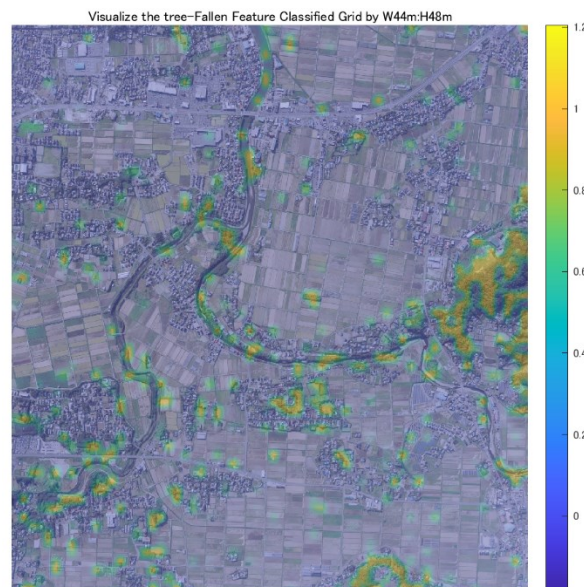
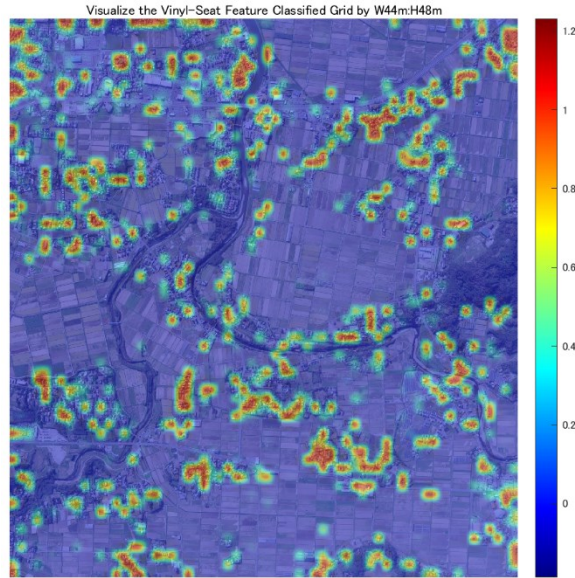
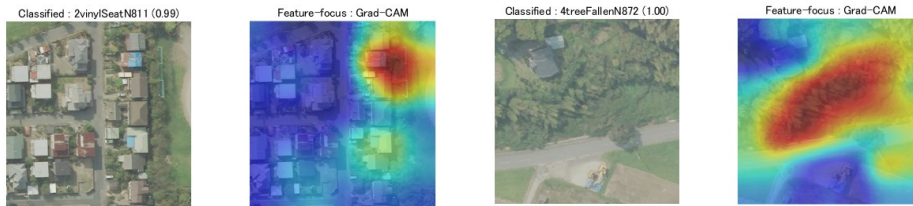
**Fig. 5.** Tree fallen feature map using damage class probabilities

Fig. 6 shows the house roof break covered with vinyl seat damage feature map computed on the class probabilities per unit grid. This colour is scaled between the blue and

red. The red side is positive roof break affected by strong wind. Here, we can visualize that many residential areas are devastated and vinyl seat remains on the house roof.



**Fig. 6.** House roof break feature map using damage class probabilities



**Fig. 7.** Visual explanation more detail scale per grid using Grad-CAM (left pair of original clip and activation map : roof break covered with vinyl seat, right pair : tree-fallen)

## 4 Concluding Remarks

### 4.1 Disaster Features Visualization for Initial Response Support

This paper proposed a method to predict the damaged area highlighted on the typhoon disaster feature such as tree-fallen and house roof break using aero-photographs images. This method was able to classify land covers without damages and with ones 64 by 64 partitioned with unit grid images of 48 meter square. Exactly, we trained the preferable deep network classifier with advantage of disaster class accuracy, the ShuffleNet compared with ten practical candidates of usable deep neural networks such as AlexNet, VGG16, GoogleNet, Inception-v3, ResNet50, ResNet101, DenseNet-201, MobileNet-

v2 and so forth. Using target class probabilities per unit grid, we were able to visualize disaster features map to scale the colour range from blue to red and yellow. Furthermore, we were able to explain the disaster features on each unit grid images to compute the convolutional activation map using Grad-CAM based on deep classification network layers. This paper demonstrated training and test studies applied to aero-photographs with the size of 14 thousands pixels by 15 thousands ones recorded at the south Chiba region after eighteen days at the post Typhoon Faxai, 27 to 28 September 2019. We confirmed that this application is available to the case of typhoon disaster for initial response support.

#### 4.2 Future Works for Disaster Visual Mining and Learning Variations

This paper studied the one of disaster features of strong wind due to typhoon. Further, we try to carry out visual data mining towards another supervised sky view images though disaster event is rare, so we need to continue to collect aerial photographs at next coming typhoon with different damage features [23], for example flooded area and levee break point. Though it needs a lot of annotation works to divide subgroup of clips, we can build a prototype of classifier and using the base model we can almost automate to classify subgroup of clips, and it remains works to check errors less than human annotation. This method is possible to develop an applications to visualize disaster features end-to-end from an input of aerial photograph into a colour scaled disaster feature map over another devastated fields. Furthermore, we can try to learn and represent various disaster features [24-26] and so it could be possible to make the visual explanation for initial response support in order to faster recovery.

**Acknowledgements.** I wish to thank Aero Asahi Co.Ltd. for providing us the aerial photographs self-recorded at the south Chiba region after Typhoon Faxai. I wish to thank Takuji Fukumoto and Shinichi Kuramoto (MathWorks Japan) for suggesting us MATLAB resources.

(Preprint Submitted April 22, 2020)

#### References

1. Chou T-Y., Yeh M-L. et al. : Disaster Monitoring and Management by the Unmanned Aerial Vehicle Technology, Wanger, W. and Szekely, B(eds.) ISPRS TC VII Symposium, Austria, Vol.XXXVIII, Part 7B, 2010.
2. JICA Survey Team : Aerial Survey Report on Inundation Damages and Sediment Disasters, 15th Jun 2016.
3. Altan, M.O. and Kemper, G. : Innovative Airborne Sensors for Disaster Management, The International Archives of Photogrammetry, Remote Sensing and Spatial Information Sciences, Volme XLI-B8, XXIII ISPRS Congress, Czech Republic, July 2016.
4. Japan Bosai Platform : <https://www.bosai-jp.org/en/member/detail/78>, last accessed 2019/11/23.
5. Kokusai Kogyo : [https://www.kkc.co.jp/english/service/base\\_technologies/sky/index.html](https://www.kkc.co.jp/english/service/base_technologies/sky/index.html), last accessed 2019/11/23.

6. PASCO : Disaster Mapping for Emergency Use, <https://www.pasco.co.jp/eng/>, last accessed 2019/11/23.
7. He, M. et al. : A 3D Shape Descriptor Based on Contour Clusters for Damaged Roof Detection Using Airborne LiDAR Point Clouds, *MDPI*, 8, 189, 2016.
8. Nex, F et al. : Towards Real-Time Building Damage Mapping with Low-Cost UAV Solutions, *MDPI, Remote Sensing*, 11, 287, 2019.
9. Liu, C-C, Nakamura, R. et al. : Near Real-Time Browseable Landsat-8 Imagery, *MDPI, Remote Sensing*, 9, 79, 2017.
10. Sheykhmousa, M. et al. : Post-Disaster Recovery Assessment with Machine Learning-Derived Land Cover and Land Use Information, *MDPI, Remote Sensing*, 11, 1174, 2019.
11. Krizhevsky, A., Ilya S., and G. E. Hinton.: ImageNet Classification with Deep Convolutional Neural Networks. *Advances in neural information processing systems*, 2012.
12. Szegedy, C., Wei L., Yangqing J., et al. : Going deeper with convolutions, in *Proceedings of the IEEE conference on computer vision and pattern recognition*, 1-9, 2015.
13. VGG model, the Visual Geometry Group at University of Oxford, Simonyan, K. et al. : A. : Very Deep Convolutional Networks for Large-Scale Image Recognition, *ICLR.*, 2015.
14. Inception v3 model, Szegedy, C., Vincent, V., Sergey, I. et al. : Rethinking the Inception Architecture for Computer Vision, *CVPR*, 2818-2826, 2015.
15. ResNet model, Kaiming, H. Xiangyu, Z., Shaoqing, R. et al. : Deep Residual Learning for Image Recognition, *arXiv:1512.03385v1*, 2015.
16. Inception-ResNet-v2 model, Szegedy, C., Sergey, I., Vincent, V. et al. : Inception-v4, Inception-ResNet and Impact of Residual Connections on Learning, 2016.
17. DenseNet model, Huang, H., Liu, Z., Maaten, L. et al. : Densely Connected Convolutional Networks, *CVPR.*, 2017.
18. Sandler, M., Howard, A. et al. : MobileNetV2: Inverted Residuals and Linear Bottlenecks, *arXiv:1801.04381v4*, 21 Mar. 2019.
19. Zhang, X., Zhou, X. et al. : ShuffleNet: An Extremely Efficient Convolutional Neural Network for Mobile Devices, *arXiv :1707.01083v2*, 7 Dec 2017.
20. Ma, N., Zhang, X. et al. : ShuffleNet V2: Practical Guidelines for Efficient CNN Architecture Design, *arXiv:1807.11164v1*, 30 Jul 2018.
21. Selvaraju, R., Cogswell, M. et al. : Grad-CAM: Visual Explanations from Deep Networks via Gradient-based Localization, *arXiv:1610.02391v3*, 21 Mar 2017.
22. Gonzalez, R., Woods, R., Eddins, S. : Digital Image Processing Using MATLAB second edition, McGrawHill Education, 2015.